SLAC-PUB-3321
April 1984
T/E

# RECENT RESULTS ON PROMPT ELECTRON PRODUCTION AT PEP*

ECKHARD ELSEN
(Representing the DELCO Collaboration[1])
*Stanford Linear Accelerator Center*
*Stanford University, Stanford, California 94305*

## ABSTRACT

Recent experimental results on production of prompt electrons in $e^+e^-$ annihilation at PEP are reviewed. The semielectronic branching ratios and the fragmentation functions of B- and C-mesons are discussed.

---

* Work supported in part by the Department of Energy contracts DE-AC03-76SF00515 and DE-AC03-83-ER-40050, the National Science Foundation and the Alexander von Humboldt Foundation.

Invited talk presented at the Rencontre de Moriond: New Particle Production, La Plagne, France, March 4-10, 1984.

## 1. Introduction

There are two main sources of prompt electrons at present $e^+e^-$-annihilation energies: the decay of mesons with b- and c-flavored quarks. In the simplest picture for this process, the b-quark, for example, decays weakly into a charm quark, emitting a virtual W, which in turn has an appreciable branching ratio into electrons. The other constituent quark of the heavy meson acts like a spectator in the process (Fig. 1). Due to the different parent quark masses, electrons from the two processes can be statistically distinguished through their distributions in $p$ and $p_T$, measured with respect to the event axis. This provides a measurement of both the semielectronic branching ratios and the momentum distributions of hadrons with heavy quarks, the latter being parameterized by the quark fragmentation function.

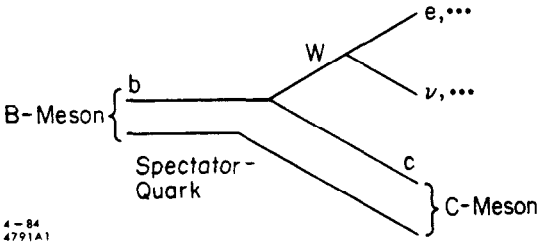


Fig. 1. Spectator diagram for the decay of a B-meson into a charmed meson and $e\nu$.

## 2. Inclusive Electron Spectrum

Previous measurements of semielectronic decays of heavy quarks had to confine the electron to regions of rather high momenta[2]. New data from PEP extend this momentum range considerably.

### 2.1 DELCO Data

The DELCO group studies the electron spectrum for $0.5 < p < 5.5$ GeV/c, covering almost the entire kinematic range. Particle momenta are measured in a drift chamber system in an open geometry magnet with a precision $\frac{\sigma_p}{p} = \sqrt{(0.02p)^2 + 0.06^2}$. Electrons in the sample of hadronic events are identified primarily by the threshold Čerenkov counter system[3] and a system of shower counters. Two separate experiments are performed by initially using isobutane and later nitrogen as a Čerenkov radiator. Electron candidates are tracks below pion threshold triggering a Čerenkov cell. In addition to the pulse height requirement, strict timing cuts are applied.

Backgrounds in the resulting electron sample come predominantly from two sources:

Real electrons These originate from Dalitz decay or $\gamma$-conversions in the material before the drift chamber entrance. They are identified by reconstruction of the $e^+e^-$ pair. A

visual scan removes most of the asymmetric conversions, where one of the tracks has very low momentum and is not found by the pattern recognition program.

Fake electrons The track is actually a hadron but the Čerenkov cell is triggered by a late $\gamma$-conversion leaving no or too few hits in the central chamber. A high fraction of these tracks can be identified through unassociated hits in the outer chambers. Finite momentum resolution causes another background of hadrons close to Čerenkov momentum threshold.

Relevant numbers for the two experiments are summarized in Table I.

Table I. DELCO Electron Analysis

| | Isobutane | Nitrogen |
|---|---|---|
| Hadrons | $33 \times 10^3$ | $9.5 \times 10^3$ |
| $\int Ldt$ [pb$^{-1}$] | 92 | 26 |
| Pion threshold [GeV/c] | 2.5 | 5.5 |
| <Čerenkov photo electrons> | 18.0 | 4.8 |
| Electron candidates | 515 | 199 |
| Background fraction | 26% | 18% |

The momentum distributions are shown in Fig. 2 together with the individual background contributions. Figure 3(a) shows the cross sections derived from this data after subtraction of residual background. Good consistency is found between the two experiments performed by DELCO. Accounting for the systematic errors, primarily due to uncertainties in the detection efficiency (9%), luminosity (5%) and background subtraction (4%) the data are combined to yield a precise measurement of the cross section over the momentum range considered [Fig. 3(b)].

The total cross section deduced in the momentum range $0.5 < p < 5.5$ GeV/c is $\sigma_{tot} = 35.8 \pm 4.6$ pb at $E_{c.m.} = 29$ GeV.

## 2.2 TPC DATA

The PEP-4 TPC group[5] identifies electrons using both the TPC-ionization loss and the energy information from the gas sampling calorimeter for particles above 0.5 GeV/c momentum. The hadron misidentification probability from the TPC alone is found to be $0.2 - 2.0\%$ above 1.5 GeV/c and 3% for $0.5 < p < 1.5$ GeV/c due to overlap between the electron band and the bands of other particles. The hadron misidentification probability in the calorimeter varies between 2.5% and 5% depending on the position of the track with respect to the core of the jet yielding a combined misidentification probability from both systems of $0.003\% - 0.3\%$ depending on both $p$ and $p_T$.

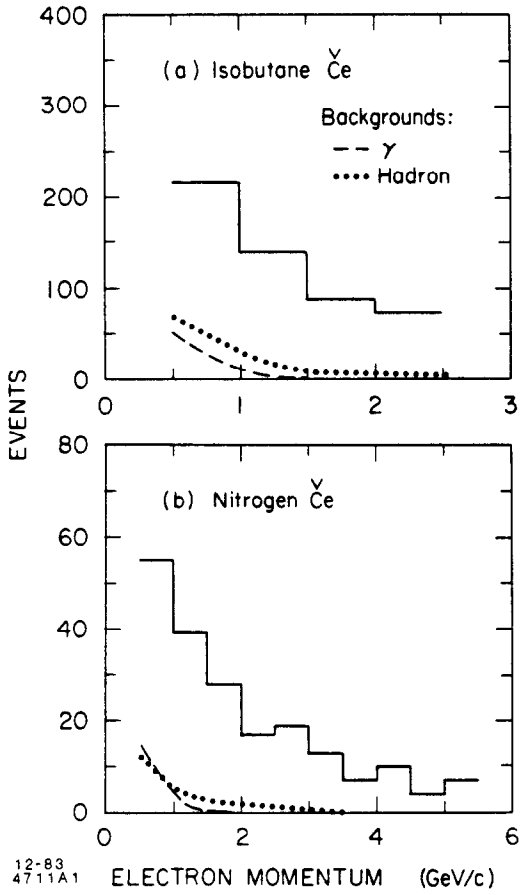


Fig. 2. Momentum spectrum of electron candidates for the the two radiator gases used.

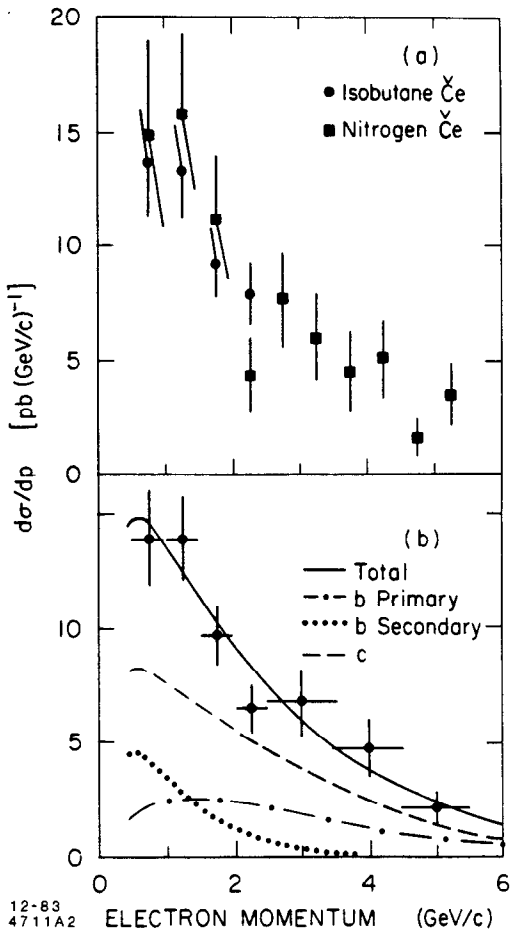


Fig. 3. Momentum spectrum of prompt electrons for (a) Isobutane and Nitrogen data and (b) the two data combined. The vertical error bars account for statistical and systematic errors. The solid line in (b) shows the fit using the fragmentation function of Ref. 4. The individual contributions from $b \to e, b \to c \to e$ and $c \to e$ are also indicated.

Background By far the largest background in this sample is caused by electrons from photons converting in the material in front of the TPC (0.2 radiation lengths). 75% of these conversions are reconstructed.

Table II. TPC Electron Analysis

| | |
|---|---|
| $\int Ldt$ [pb$^{-1}$] | 77 |
| Electron candidates | 819 |
| Background fraction for $p > 1$ GeV/c | $\approx 30\%$ |

The individual backgrounds are subtracted using the distributions from the Monte Carlo simulation. The error of the cross section measurement is dominated by the uncertainty in the estimate of the conversion background at low momenta and of the detection efficiency of the calorimeter at high momenta. Figure 4 shows the inclusive electron cross section of the PEP experiments. Good agreement is found between the different experiments.

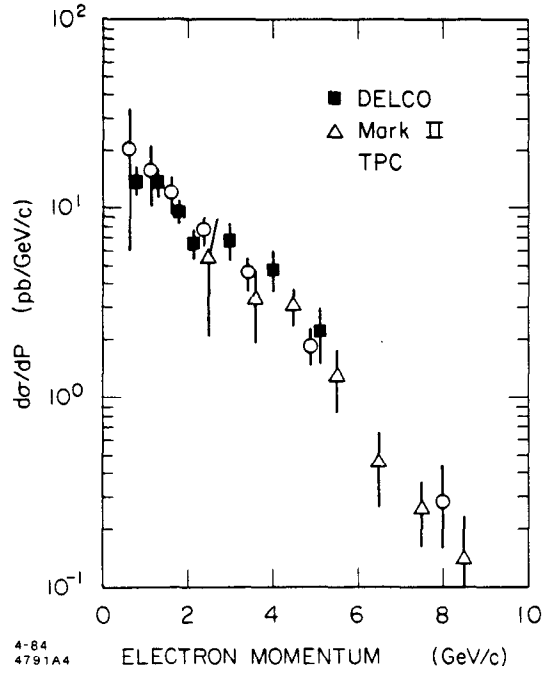


Fig. 4. Inclusive electron cross section.

## 3. Branching Ratios and Fragmentation Functions

The branching ratios and the fragmentation functions are determined from a two-dimensional fit to the distributions in $p$ and $p_T$ using the LUND Monte Carlo[6] to relate the heavy quark momentum distributions to the electron distribution. The TPC group analyze their data for $p > 1$ GeV/c assuming a fixed shape for the charm fragmentation function, whereas DELCO determines both branching ratios and fragmentation function from a fit to the entire momentum range measured. Among other functional forms both experiments use the ansatz of Ref. 4 for the heavy quark fragmentation function, which yields semielectronic branching ratios as summarized in Table III.

Good agreement is found between the measurement of branching ratios from the different experiments. The result is insensitive to different assumptions on the shape of the fragmentation function. The branching ratios for b-quarks are compared to earlier measurements[8] including those from lower $c.m.$ energies[9] in Fig. 5.

Both experiments find little sensitivity to measure the actual shape of the fragmentation function but establish high average values for the fragmentation variable[10] $z$.

Table III. Results of Fits to Electron Distributions[7]

| | DELCO | TPC |
|---|---|---|
| BR(b) | $14.8 \pm 2.8\%$ | $11.0 \pm 1.8 \pm 1.0\%$ |
| BR(c) | $9.0 \pm 1.3\%$ | $9.1 \pm 0.9 \pm 1.3\%$ |
| $< z_b >$ | $0.78 \pm 0.05$ | $0.74 \pm 0.05 \pm 0.03$ |
| $< z_c >$ | $0.69 \pm 0.06$ | -- |

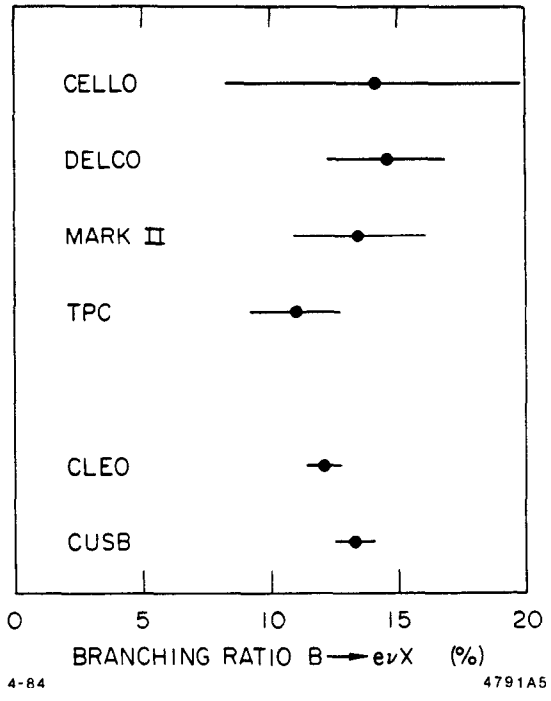


Fig. 5. Comparison of measurements of semielectronic b-branching fractions from different experiments.

## 4. B-Events

The $p$ and $p_T$ spectrum of the electrons from DELCO is shown in Figs. 3(b) and 6, together with the best fit result of the Monte Carlo using the function of Ref. 4. For $p_T >$ 1 GeV/c, more than 80% of the electrons originate from b-decays. The following analysis uses this possibility of tagging b-events to investigate the properties of the jet opposite to the high $p_T$ electron. Figure 7 displays the invariant mass observed in the hemisphere of the electron and in the opposite hemisphere, where the hemispheres are defined by the thrust axis in the event. The distributions are compared to the invariant mass calculated

from charged particles in a hemisphere of the average hadronic event. The hemisphere containing the high $p_T$ electron favors larger masses than the average event because of the selection procedure. The mass distribution in the opposite hemisphere, however, also exhibits somewhat larger values.

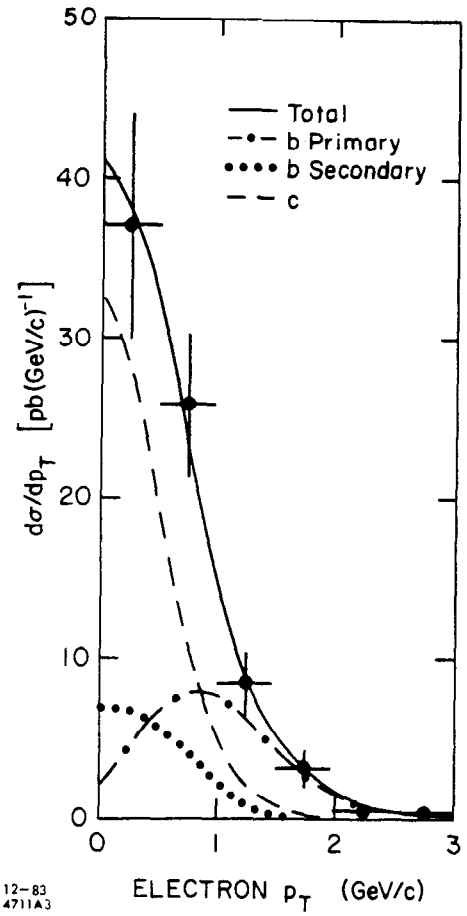


Fig. 6. $p_T$ spectrum of electrons together with the result of the best fit indicating the different sources of electrons.

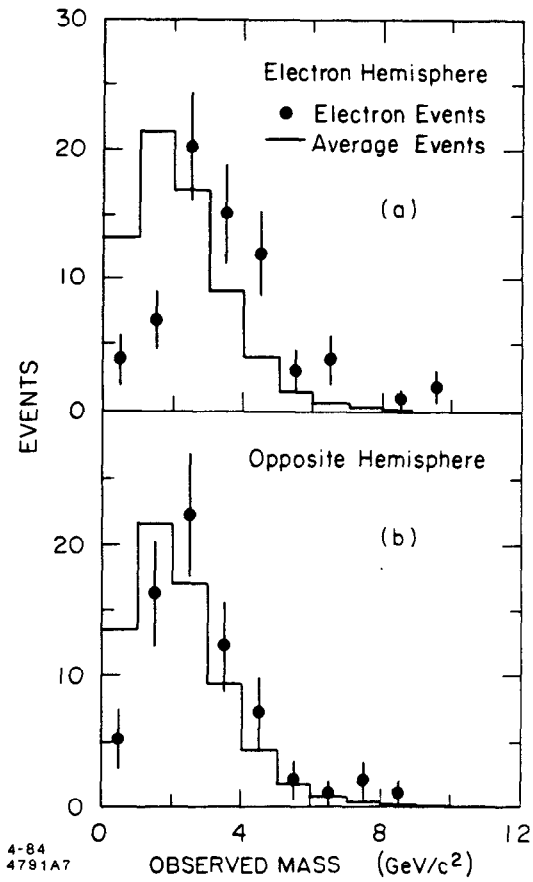


Fig. 7. Observed mass in (a) the hemisphere of the high $p_T$ electron and (b) the opposite hemisphere compared to the invariant mass of a hemisphere in the average hadronic event. Invariant masses in all cases are calculated using charged particles only.

The rapidity distribution of the particles in electron events and average events is compared in Fig. 8. The rapidities of particles in both the hemisphere of the electron and the opposite hemisphere extend to smaller values than in the average event.

These observations are in agreement with the expectations for the production of massive B-particles in both jets, one of them being detected by an electron with high transverse momentum and the other effectively reducing the rapidity range available for the decay particles.

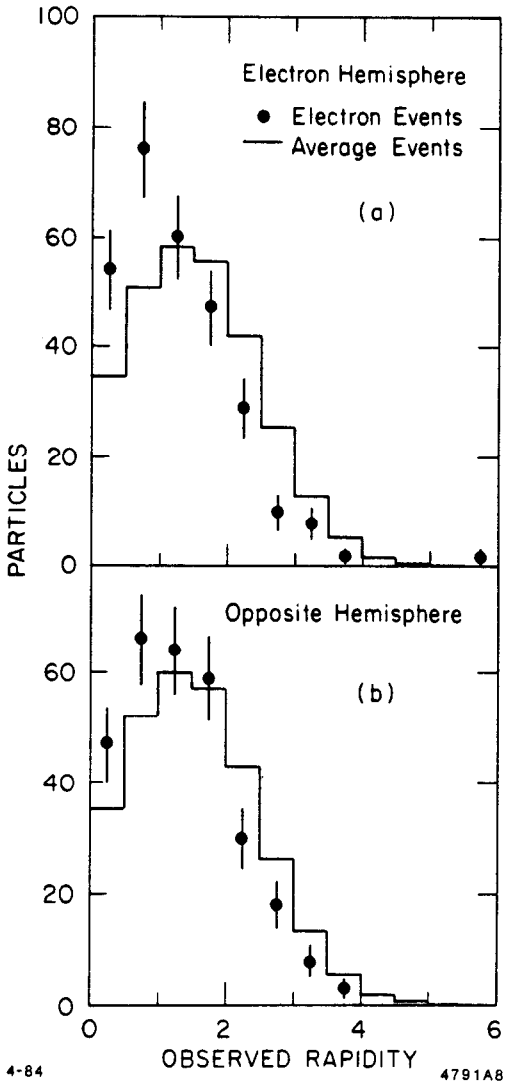


Fig. 8. Observed rapidity of charged particles in (a) the hemisphere of the high $p_T$ electron and (b) the opposite hemisphere compared to the rapidity of particles in the average hadronic event.

## REFERENCES

1. The members of the DELCO collaboration are: W. B. Atwood, P. H. Baillon, B. C. Barish, G. R. Bonneaud, A. Coureau, H. DeStaebler, G. J. Donaldson, R. Dubois, M. M. Duro, E. E. Elsen, S. G. Gao, Y. Z. Huang, G. M. Irwin, R. P. Johnson, H. Kichimi, J. Kirkby, D. E. Klem, D. E. Koop, J. Ludwig, G. B. Mills, A. Ogawa, T. Pal, D. Perret-Gallix, R. Pitthan, D. L. Pollard, C. Y. Prescott, L. Z. Rivkin, L. S. Rochester W. Ruckstuhl, M. Sakuda, S. S. Sherman E. J. Siskind, R. Stroynowski, S. Q. Wang, S. G. Wojcicki, H. Yamamoto, W. G. Yan, C. C. Young.

2. M.E. Nelson et al., Phys. Rev. Lett. 50, 1542 (1983).

3. J. Kirkby, Proceedings of the 21st International Conference on High Energy Physics, Journal de Physique, 43, C3-45 (1982). G. Gidal et al., Berkeley Particle Data Group, LBL-91, supplement UC-37 (1983).

4. C. Peterson et al., Phys. Rev. D 27, 105 (1983).

5. See talk by R. Madaras at this meeting.

6. T. Sjoestrand, Comput. Phys. Commun. 27, 243 (1982) and Comput. Phys. Commun. 28, 229 (1983).

7. In the case of DELCO systematic effects are accounted for through additional variable factors in the likelihood function. They are included in the quoted errors. The TPC numbers refer to statistical and systematical error separately.

8. H.J. Behrend et al., Z. Phys. C19, 291 (1983); D. Koop et al., SLAC-PUB-3266, December 1983; G. Hanson, SLAC-PUB-3194, August 1983.

9. C. Klopfenstein et al., Phys. Lett. 130B, 444 (1983); A. Chen et al., CLEO Collaboration, preprint CLNS-84/597, February 1984.

10. The DELCO group uses a definition $z = 2E_H/\sqrt{s}$ where $\sqrt{s}$ is the energy of the virtual photon after accounting for initial state radiation, TPC assumes $z = E_H/E_{beam}$. DELCO finds that the effect of the initial state photon radiation is to reduce $< z >$ by $2-4\%$.